Purdue University
Purdue e-Pubs

International Refrigeration and Air Conditioning Conference

School of Mechanical Engineering

2010

1-D Modeling Of Supersonic Carbon Dioxide Two-Phase Flow Through Ejector Motive Nozzle

Wojciech Angielczyk
Université Catholique de Louvain UCL

Yann Bartosiewicz
Université Catholique de Louvain UCL

Dariusz Butrymowicz
Institute of Fluid-Flow Machinery of Polish Academy of Sciences

Jean-Marie Seynhaeve
Université Catholique de Louvain UCL

Follow this and additional works at: http://docs.lib.purdue.edu/iracc

Angielczyk, Wojciech; Bartosiewicz, Yann; Butrymowicz, Dariusz; and Seynhaeve, Jean-Marie, "1-D Modeling Of Supersonic Carbon Dioxide Two-Phase Flow Through Ejector Motive Nozzle" (2010). *International Refrigeration and Air Conditioning Conference.* Paper 1102.
http://docs.lib.purdue.edu/iracc/1102

This document has been made available through Purdue e-Pubs, a service of the Purdue University Libraries. Please contact epubs@purdue.edu for additional information.
Complete proceedings may be acquired in print and on CD-ROM directly from the Ray W. Herrick Laboratories at https://engineering.purdue.edu/Herrick/Events/orderlit.html

1-D Modeling of Supersonic Carbon Dioxide Two-Phase Flow through Ejector Motive Nozzle

Wojciech ANGIELCZYK[1]*, Jean Marie SEYNHAEVE[1], Dariusz BUTRYMOWICZ[2], Yann BARTOSIEWICZ[1]

[1]Université catholique de Louvain UCL, Institute of Mechanics. Materials and Civil Engineering (iMMC)
Gdańsk, Poland,
butrym@imp.gda.pl

* Corresponding Author

ABSTRACT

A promising device which could help to reduce losses and improve efficiency of CO2 transcritical refrigeration cycle, is the ejector technology. However, modeling such a device is really challenging because not only the transcritical nature of the flow but also the occurrence of a choked flow rate, where thermodynamics equilibrium is a big issue. The two-phase critical flow of a carbon dioxide through ejector motive nozzle is modeled by means of the Homogenous Relaxation Model (HRM). Existing closure laws for relaxation time were adapted for carbon dioxide. The pressure distribution along the nozzle is calculated for three different nozzle geometries and compared with an experimental data. The issue of the sound velocity is discussed in terms of differences between prediction accuracy of Homogenous Equilibrium Model (HEM) and HRM.

1. INTRODUCTION

One of the most important efficiency losses in the refrigeration system, especially in a transcritical CO_2 cycle, is caused by the throttling process. The most promising solution is the application of a two-phase ejector as a compressor booster. The schematic and the thermodynamic diagram of this solution is presented in

Figure 1: Vapor compression transcritical refrigeration device equipped with the two-phase ejector
a) Schematic diagram b) Thermodynamic cycle in pressure-enthalpy diagram

Figure 1. The ejector operqtion can be described as following. Liquid refrigerant flows from cooler to the motive nozzle of ejector where it expands from pressure of point 3 to the pressure of point 3` (Figure 1). The further expansion causes partial evaporation of refrigerant, as a result the two-phase mixture flows from the outlet of the motive nozzle. This motive stream entrains the vapor from the evaporator. Both streams are mixed in mixing chamber. The path between point 5 and point 6 represents change of vapor stream state in mixing process while the path 4-6 represents change of motive stream state. During the mixing process the refrigerant is partly compressed due to a mixing shock, so the pressure increases from the evaporation pressure to the pressure of point 6. The path between point 6 and 7 represents the compression process in diffuser. As a result of the two-phase ejector, suction pressure at the compressor is higher than in case of a standard system equipped with a throttling device. Therefore the ejector-compression cycle requires less energy.

In this nozzle, the total energy is conserved but the potential energy of pressure at inlet is partly converted into kinetic energy. The lower the pressure is at the motive nozzle outlet, the higher the motive stream velocity is, providing a better potential of momentum exchange with the secondary stream farther downstream. For given operating conditions (inlet, outlet pressure) the maximum achievable velocity for a simple converging nozzle is the propagation velocity or the speed of sound. For a converging-diverging nozzle, the velocity at the nozzle outlet could be larger and depends on the divergent design. Therefore, an accurate prediction of local speed of sound values is a crucial issue for a nozzle design.

Figure 2 shows the influence of the two-phase flow quality on the sound speed of CO_2, under two different pressures: p= 6.6995 MPa close to the critical pressure and for a relatively low pressure - p=3.6829 MPa. It is easy to see that predictions of HRM and HEM differ very much, especially for low qualities, which are expected to occur at the motive nozzle throat (Henry and Fauske, 1971, Nakagawa, 2009). For saturated liquid CO_2 at 6 .6995 MPa the REFPROP subroutines (1980) gives the value of sound speed equals to 247.13 m/s, which is consistent with predictions of HRM but completely inconsistent with results of HEM. Similar situation appears for 3.6829 MPa when for saturated liquid CO_2 the REFPROP database (1980) pointes out 516.78 m/s. Consequently, HRM seems to be more appropriate for critical flow calculations of the motive nozzle. It should be emphasize that in HEM the specific enthalpy and the sound velocity are functions only of two variables (in this case: p and $\bar{x}$) while in HRM the sound velocity is a function of three variables (p, h_{ML} and x). Therefore to calculate the sound velocity for HRM it was assumed that at each point the specific enthalpy h is the same for both models. Based on this assumption and equation (6b), the value of the metastable liquid fraction enthalpy h_{ML} was calculated.
Attou and Seynhaeve (1999) investigated the steady-state critical two-phase flashing flow with possible multiple choking phenomenon. They compared results obtained from HEM and Delayed Equilibrium Model (DEM) for water flow. They found a high deviation of predicted sound speeds between both models and they also concluded that HEM is not appropriate to predict the sound speed for low quality flows.

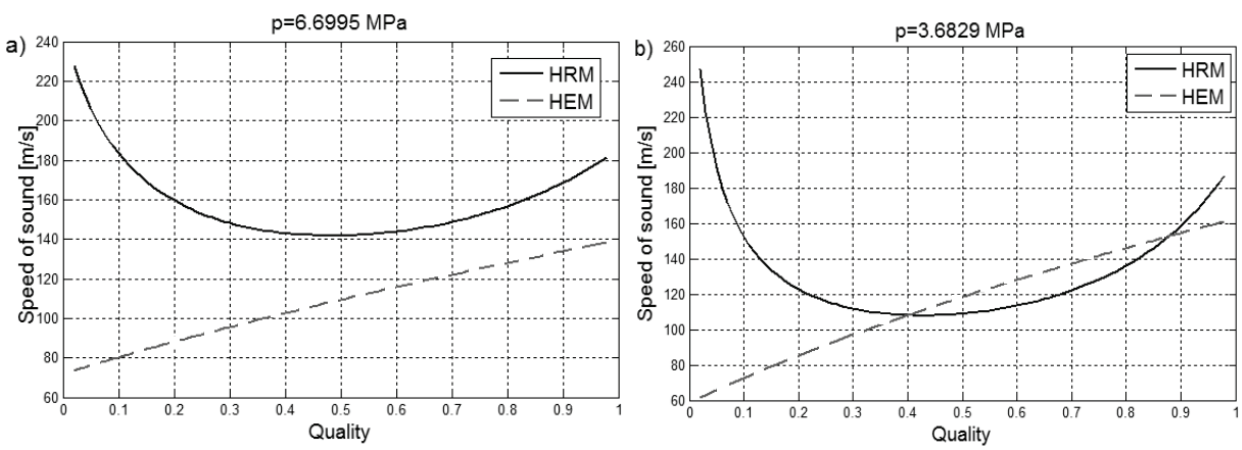

Figure 2: Influence of the two-phase flow quality on the CO_2 speed of sound: a) 6.6995 MPa; b) 3.6829 MPa

2. HOMOGENEOUS RELAXATION MODEL OF MOTIVE NOZZLE TWO-PHASE FLOW

The idea of HRM comes form the fact that an instantaneous thermodynamic equilibrium between each phase cannot exist. During the process of phase change, the local instantaneous quality x may be different from its value at equilibrium (saturation) $\bar{x}$. In the model, this metastability is governed by a relaxation equation.

2.1 Equation system and solving procedure

The HRM is constructed on a base of four equations (Bilicki,1990): the mass conservation equation- Equation (1), the momentum conservation equation- Equation (2), the energy conservation equation- Equation (3), and the vapor mass balance equation- Equation (4). The system can be cast in one dimension:

$$\frac{\partial \rho}{\partial t} + w\frac{\partial \rho}{\partial z} + \rho\frac{\partial w}{\partial z} = -\rho w\frac{1}{A}\frac{\mathrm{d}A}{\mathrm{d}z} \tag{1}$$

$$\rho\frac{\partial w}{\partial t} + \rho w\frac{\partial w}{\partial z} = \rho g\cos\beta - \frac{\tau C}{A} - \rho\frac{\partial p}{\partial z} \tag{2}$$

$$\rho\frac{\partial h}{\partial t} - \frac{\partial p}{\partial t} + \rho w\frac{\partial h}{\partial z} - w\frac{\partial p}{\partial z} = w\frac{\tau C}{A} + \frac{qC}{A} \tag{3}$$

$$\frac{\partial x}{\partial t} + w\frac{\partial x}{\partial z} = -\frac{x-\bar{x}}{\Theta} \tag{4}$$

Assuming that flow inside the motive nozzle is a steady adiabatic horizontal flow, that the depended variables are elements of following state-velocity vector:

$$\sigma = \left[p, h_{ML}, x, w\right]^T, \tag{5}$$

and that the specific volume and the specific enthalpy are given as:

$$v_{ML} = xv_{SG}(p) + (1-x)v_{ML}\left(p, h_{ML}\right), \qquad h = xh_{SG}(p) + (1-x)h_{ML} \tag{6a, b}$$

the system of the HRM can be reduced by using Cramer method:

$$\frac{\mathrm{d}p}{\mathrm{d}z} = \frac{\Delta_p}{\Delta}, \qquad \frac{\mathrm{d}h_{ML}}{\mathrm{d}z} = \frac{\Delta_{h_{ML}}}{\Delta}, \qquad \frac{\mathrm{d}x}{\mathrm{d}z} = \frac{\Delta_x}{\Delta}, \qquad \frac{\mathrm{d}w}{\mathrm{d}z} = \frac{\Delta_w}{\Delta}, \tag{7a, b, c, d}$$

where:

$$\Delta = w\left(a_2 M + E_2 a_1\right), \qquad \Delta_p = MTA_4 - wA_3, \qquad \Delta_{h_{ML}} = a_1 A_8 + M\left(TA_9 + wA_{10}\right), \tag{8a, b, c}$$

$$\Delta_x = -\frac{T}{w}\Delta, \qquad \Delta_w = -TA_4 - w\left(a_3 + FA_{12}\right). \tag{9a, b}$$

$$a_1 = \frac{1}{M}, \qquad a_2 = C_1 E_2 - C_2 E_1, \qquad a_3 = \frac{E_2}{\rho A}\frac{\mathrm{d}A}{\mathrm{d}z}, \qquad a_4 = \frac{ME_2}{\rho A}, \qquad a_5 = \frac{E_1}{\rho A}, \tag{10a, b, c, d, e}$$

$$A_1 = C_1 M + a_1, \qquad A_2 = a_2 - E_2 a_1^2, \qquad A_3 = M\left(C_2 F - a_3\right) + E_2 F a_1, \tag{11a, b, c}$$

$$A_4 = C_3 E_2 - C_2 E_3, \qquad A_5 = C_2 F - a_3 - E_2 F a_1^2, \qquad A_6 = Fa_1 - \frac{M}{\rho A}\frac{\mathrm{d}A}{\mathrm{d}z} \tag{12a, b, c}$$

$$A_7 = MC_2 + E_2 a_1, \qquad A_8 = wF\left(1 + E_1\right) + E_3 T, \qquad A_9 = C_1 E_3 - C_3 E_1 \tag{13a, b, c}$$

$$A_{10} = C_1 F - a_5 \frac{\mathrm{d}A}{\mathrm{d}z}, \qquad A_{11} = C_1 E_2 - C_2 (1 + E1) \tag{14a, b}$$

$$C_1 = x \frac{\mathrm{d}v_{SG}}{\mathrm{d}p} + (1 - x) \frac{\partial v_{ML}}{\partial p}, \qquad C_2 = (1 - x) \frac{\partial v_{ML}}{\partial h_{ML}}, \qquad C_3 = v_{SG} - v_{ML}. \tag{15a, b, c}$$

$$E_1 = \rho x \frac{\mathrm{d}h_{SG}}{\mathrm{d}p} - 1, \qquad E_2 = \rho (1 - x), \qquad E_3 = \rho \left(h_{Sg} - h_{ML}\right), \tag{16a, b , c}$$

$$F = \frac{\tau C}{A}, \qquad M = \rho w, \qquad T = \frac{x - \overline{x}}{\theta} \tag{17a, b, c}$$

The equation system similar to system (1÷4) was investigated by Bilicki et al. (1990). It was proven that the system has a saddle singular point at critical section. The coordinates z_s, σ_s of singular point can be obtained by using two equations:

$$\Delta(\sigma_s) = 0 \qquad \Delta_i(z_s, \sigma_s) = 0, \tag{18a, b}$$

where: $i \in \left\{p, h_{ML}, w\right\}$. Therefore the left hand-side of equation (18b) can be freely chosen among three secondary determinants of the differential equations system, but it cannot be Δ_x. This secondary determinant is always equals 0 when the system determinant Δ is equal (equation (9a)). Thus the condition $\Delta_x = 0$ is identical with the condition given in equation (18a). If three variables are assumed (e.g. (z, p, x)), remaining two other variables (e.g. (h_{ML}, w) are given by solution of equation system (18). If equation system (18) is not fulfilled assumed variables need to be changed iteratively.

The passage through the saddle point during a numerical integration from the nozzle inlet towards the nozzle outlet is technically impossible. Indeed, in the neighborhood of a singular point, even small numerical errors cause significant changes of trajectories. Nevertheless the integration can be initiated from the singular point neighborhood and continued towards the motive nozzle inlet or towards the motive nozzle outlet. In this case, the integration path has to follow one of directions defined by eigenvectors, which are themselves related to two not vanishing real eigenvalues of a following jacobian matrix:

$$J = \begin{bmatrix} 0 & \frac{\partial \Delta}{\partial p} & \frac{\partial \Delta}{\partial h_{ML}} & \frac{\partial \Delta}{\partial x} & \frac{\partial \Delta}{\partial w} \\ \frac{\partial \Delta_p}{\partial z} & \frac{\partial \Delta_p}{\partial p} & \frac{\partial \Delta_p}{\partial h_{ML}} & \frac{\partial \Delta_p}{\partial x} & \frac{\partial \Delta_p}{\partial w} \\ \frac{\partial \Delta_{h_{ML}}}{\partial z} & \frac{\partial \Delta_{h_{ML}}}{\partial p} & \frac{\partial \Delta_{h_{ML}}}{\partial h_{ML}} & \frac{\partial \Delta_{h_{ML}}}{\partial x} & \frac{\partial \Delta_{h_{ML}}}{\partial w} \\ 0 & \frac{\partial \Delta_x}{\partial p} & \frac{\partial \Delta_x}{\partial h_{ML}} & \frac{\partial \Delta_x}{\partial x} & \frac{\partial \Delta_x}{\partial w} \\ \frac{\partial \Delta_w}{\partial z} & \frac{\partial \Delta_w}{\partial p} & \frac{\partial \Delta_w}{\partial h_{ML}} & \frac{\partial \Delta_w}{\partial x} & \frac{\partial \Delta_w}{\partial w} \end{bmatrix}, \tag{19}$$

but in this case the system of differential equations needs to be transformed into following form:

$$\frac{\mathrm{d}z}{\mathrm{d}l} = \Delta \qquad \frac{\mathrm{d}p}{\mathrm{d}l} = \Delta_p \qquad \frac{\mathrm{d}h_{ML}}{\mathrm{d}l} = \Delta_{h_{ML}} \qquad \frac{\mathrm{d}x}{\mathrm{d}l} = \Delta_x \qquad \frac{\mathrm{d}w}{\mathrm{d}l} = \Delta_w, \tag{20}$$

where l is an arbitrary parameter used as a new path-variable of integration .

2.2 Modeling of metastable liquid properties

The quantities denoted by ML subscript are related with the metastable fraction of the fluid. The specific volume of the metastable liquid is obtained by an extrapolation of the isochors of the subcooled liquid into a two-phase region. The specific volume of metastable liquid is indicated for given pressure *p* and meta stable liquid specific enthalpy h_{ML} in way shown on Figure 3 (both quantities *p* and h_{ML} are elements of the vector σ thus they are obtained during solution process). Metastable liquid isochors are extrapolated into two-phase region by means of third order spline functions.

The value of the quality at the unconstrained-equilibrium state $\overline{x}$ is calculated like in HEM but based on the values of pressure *p* and enthalpy *h* given in equation (6b).

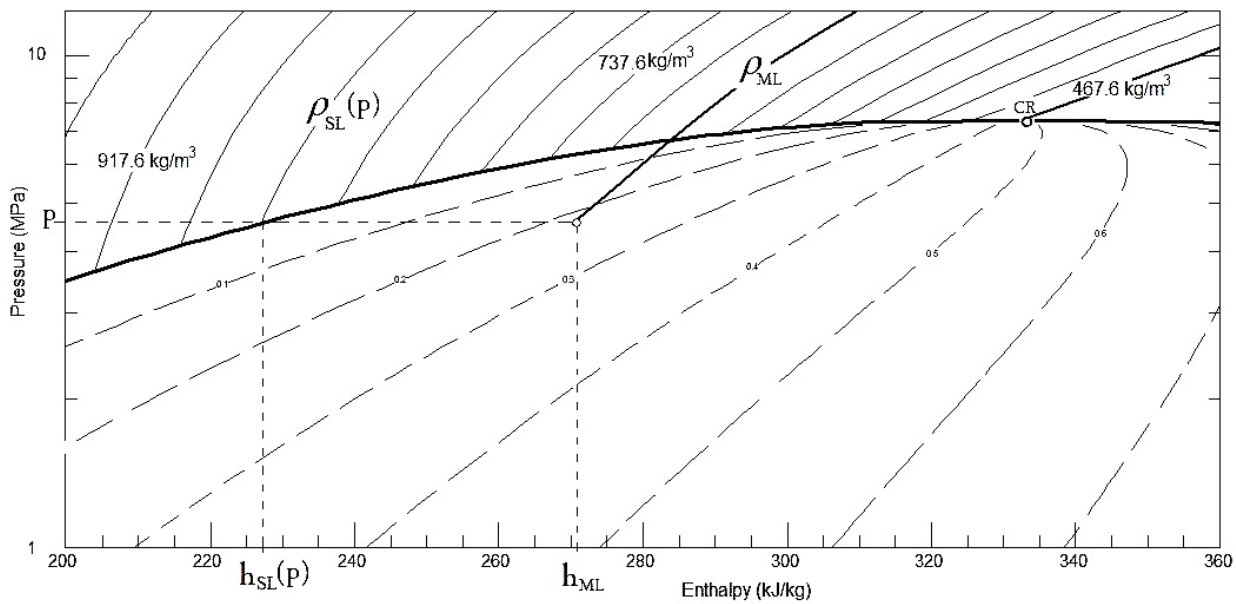

Figure 3: Indication procedure of metastable fraction specific volume

2.3 Closure laws

The relaxation time was modeled by correlation developed for water by Downar-Zapolski et al. (1996) according the Moby Dick and Super Moby Dick experiments (1974):

$$\Theta = \Theta_0 \left(x \frac{v_{SG}}{v} \right)^a \left(\frac{p_0 - p}{pc - p_0} \right)^b \tag{21}$$

In order to adjust this law for CO_2 first calculations were made and results were compared to experimental data obtained by Nakagawa (2009). The comparison of first results reveals high deviation between modeling results and experimental data. In general, a decrease of the relaxation time improved an agreement with experimental data. Thus Θ_0 was decreased from 3.848×10^{-7}s to 2.14×10^{-7}s . Residual coefficient remains unchanged (a=-0.54, b=-1.76)

In original work of Downar-Zapolski et al. (1996) p_0 is the saturation pressure at the at inlet temperature. However this point is not defined for a supercritical inlet, so it was assumed that this is the pressure of the point which is located on the saturated liquid line and has the same specific entropy than the point characterized by p, v and x. This choice is purely arbitrary and would require special care in future researches.

The friction pressure drop was calculated by using Martinelli-Nelson-Lockhart method supported by Chisholm's empirical equation (1967).

3. RESULTS

The available experimental data concerning two-phase supercritical carbon dioxide flow trough a nozzle come from Nakagawa (2009). The experiment was made through blown-down test of CO_2. The nozzle was fed from CO_2 tank and after passing trough the nozzle, CO_2 flows out to the atmosphere. Converging-diverging stainless steel nozzles were used in the experiment. All used nozzles were rectangular with a throat area of 0.24 mm * 3 mm. During all test, the width of the nozzle (3mm) and the lengths of converging and diverging sections (27.35 mm, 56.15 mm) were unchanged. Divergence angle was changed, and for each nozzle geometry, the pressure distribution in the diverging nozzle section was measured by means of four strain gauges.

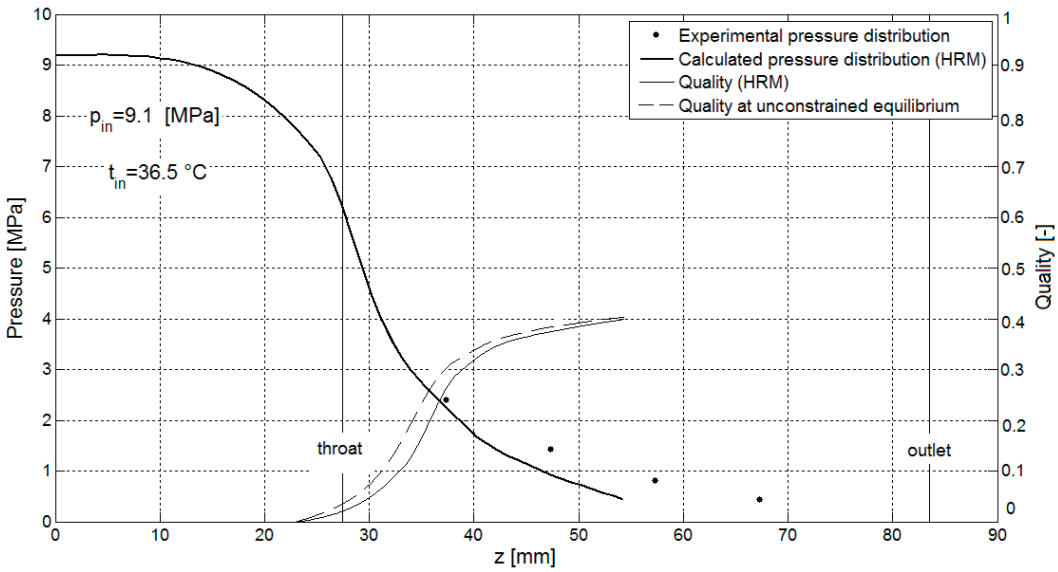

Figure 4: Comparison of experimental data with calculation results; divergence angle= 0.612°

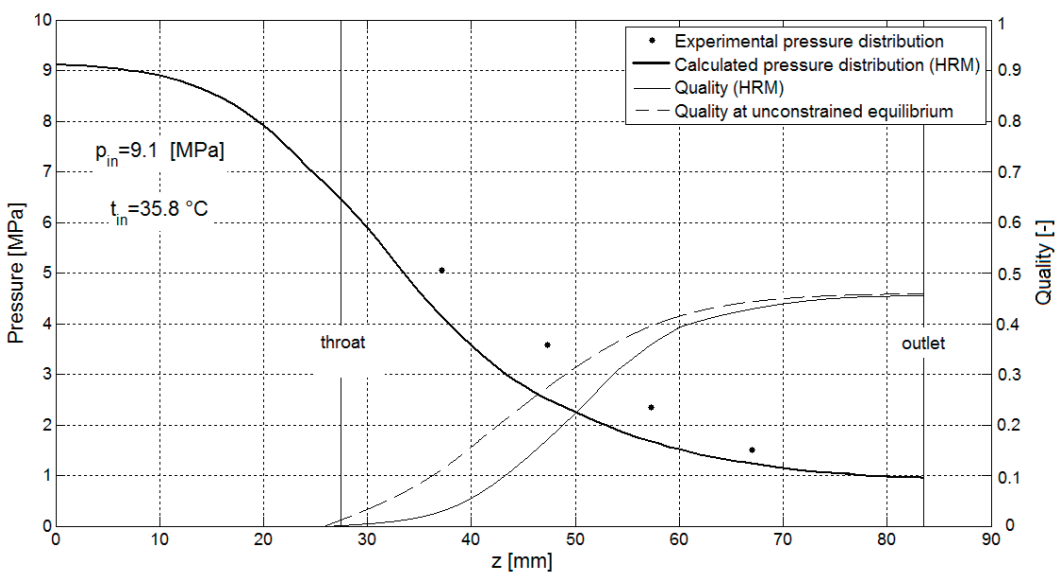

Figure 5: Comparison of experimental data with calculation results; divergence angle= 0.306°

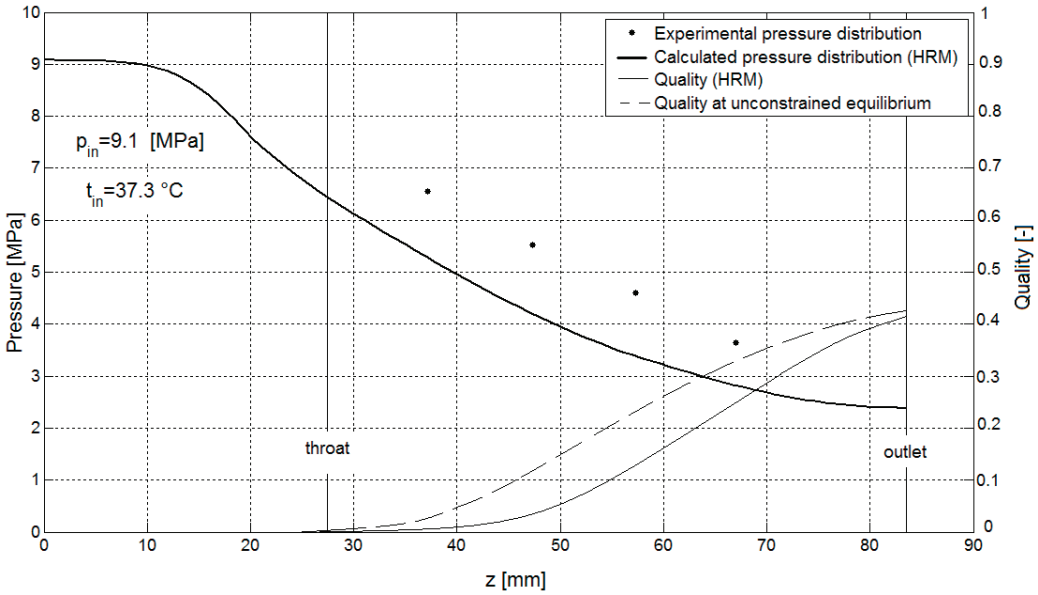

Figure 6: Comparison of experimental data with calculation results; divergence angle= 0.153°

The comparison of the experimental data (from abovementioned experiment) with calculations made on the base of previously described HRM model is presented on Figures 4, 5 and 6.

Figure 4 presents the measured and calculated pressure distribution for the nozzle with divergence angle equals 0.612 °. It could be noted that the calculated pressure profile does not cover the full range of axial positions along the nozzle but is cutoff about $z = 55\,mm$. This is due to the lower limit of validity of CO2 thermophysical properties in REFPROP database (1980). It can be observed from figure 4 that the calculated pressure decreases very quickly especially in the neighborhood of the throat. In this case experimental data cannot confirm this trend or allow to evaluate the accuracy of the model since no measurement was available upstream of the throat. However, the pressure profile calculated in the divergent section agrees well with the measured profiles (Figure 4). Figure 4 also depicts the actual and the equilibrium quality which is a direct measurement of the metastability. This non equilibrium parameter (relative difference between both quality) can reach values as high as 100% in the divergent and tend to decrease downstream where equilibrium between phases is building up.

For smaller divergent angles (Figures 5, 6), larger discrepancies are observed for the pressure profiles with a maximum difference of 28% for an angle equal to 0.306° and 27% for 0.153°. However those observed discrepancies could be related to the inadequacy of the present correlation for the relaxation time (correlated to water-steam) and also possible 2D-3D effect which cannot be captured by a 1D model. In addition, the degree of non equilibrium remains more important along the nozzle than that observed at a wider angle (Figure 4); and this becomes more important as the divergent angle is reduced (Figures 5, 6). Therefore a wider divergent seems to promote a better exchange between phases giving rise to thermodynamic equilibrium over a shorter distance.

4. CONCLUSIONS

The homogeneous relaxation model of the CO_2 supersonic two-phase flow through the ejector motive nozzle was developed. This model is clearly more consistent than the HEM in terms of propagation velocity and hence in terms of speed of sound prediction. This issue is very important since it determines the correct mass flow rate which is a key parameter of ejector operation. Pressure distributions obtained on the base of this model were compared with experimental data. Results agree reasonably well with measurements downstream the throat. However, additional experimental data in terms of number of pressure taps all along the nozzle (convergent and divergent sections), and extra information such as temperature profiles, quality profiles, and critical flow rate would be required to really assess the model and propose a suitable correlation for the relaxation time. In the near future, the model will be extended to the whole ejector geometry in an integrated model and validated with experimental data required to derive the necessary correlations.

NOMENCLATURE

The nomenclature should be located at the end of the text using the following format:

A	cross section area	(m^2)
C	perimeter	(m)
D	diameter	(m)
T	temperature	(°C)
g	gravitational acceleration	(m/s^2)
h	specific enthalpy	(J/kg)
l	dummy parameter	(-)
p	pressure	(Pa)
t	time	(s)
v	specific volume	(m^3/kg)
w	velocity	(m/s)
x	quality	(-)
$\bar{x}$	quality at unconstrained equilibrium	(-)
z	coordinate measured along the flow point	(m)
β	inclination angle	(rad)
Δ	main determinant of the differential equations system	(s/m)
Δ_i	secondary determinant of the differential equations system	
ρ	density	(kg/m^3)
Θ	relaxation time	(s)
τ	shearing stress	(Pa)

Subscripts

i	pressure, meta-stable liquid fraction specific enthalpy, quality, velocity
in	motive nozzle inlet
s	saddle point
ML	metastable liquid
out	motive nozzle outlet
SG	saturated gas
SL	saturated liquid

REFERENCES

Attou, A, Seynhaeve, J.M, 1999, Steady-state critical two-phase flashing flow with possible multiple choking Part 1: Physical modelling and numerical procedure, *Journal of Loss Prevention in the Process Industrie*s, vol. 12, no. 5: p. 335–345.

Chisholm, D., 1967, A theoretical basis for the Lockhart-Martinelli correlation for two-phase flow, *Int. J. of Heat and Mass Transfer*, vol: 10, no: 12: p.1767-1778.

Downar-Zapolski, P., Bilicki, Z., Bolle, E., Franco, J., 1996, The Non-Equilibrium Relaxation Model for One-Dimensional Flashing Liquid Flow*, Int. J. Multiphase Flow*, Vol. 22, No. 3, p. 473-483.

Henry, R., E., Fauske, H., K., 1971, The Two-Phase Critical Flow of One-Component Mixture in Nozzles, Orifices, and Short Tubes, *J. of Heat Transfer*, vol. 93, no. 2: p. 179-187.

Nakagawa, M., Berana, M., S., 2009, Supersonic two-phase flow of CO2 through converging–diverging nozzles for the ejector refrigeration cycle, *Int. J. Refrig,* vol.32, , p.1195-1202.

Bilicki, Z., Kestin, J., 1990, Physical aspects of the relaxation model in two-phase flow*, Proceedings of the Royal Society of London*, The Royal Society, A428, p. 379-397.

Réocreux, M. 1974, Contribution á l'étude des debits critiques en écoulement diphasique eau-vapeur, PhD thesis, Université Scientifique et Médicale de Grenoble, Grenoble, France.

NIST Standart Reference Database 23 1980. NIST Thermodynamics and Transport Properties of Refrigerant Mixtures, REFPROP, Version 6.01.